International Symposium of Research Students on Materials Science and Engineering
December 20-22, 2004, Chennai, India
Department of Metallurgical and Materials Engineering Indian Institute of Technology, Madras

SURFACE MODIFICATION OF MARTENSITIC STAINLESS STEEL USING METAL WORKING CO_2 LASER

Vamsi Chaitanya Bommi[1], M. Krishna Mohan[2] and Satya Prakash[1]
[1]*Department of Metallurgical and Materials Engineering,*
Indian Institute of Technology-Roorkee,
Roorkee 247667, India
[2]*Dept. of Metallurgical Engineering, NIT-Warangal, INDIA-506004.*

ABSTRACT

Surface modification of X20Cr13 martensitic stainless steel was achieved by laser surface melting using a metal working CO_2 laser. Experiments were designed to study the effect of the processing variables (Laser power, hardening (scanning) speed, and pre hardening surface condition) on the final hardness of the modified surface. The effects on the micro structural changes, macro and micro hardness were investigated by means of scanning electron microscopy, X-ray diffraction, hardness testing. Results indicate that the hardened layer of a few 100μm thick, composed of martensite with retained austenite and fine carbides was formed during the surface treatment. The hardness of the stainless steel has increased significantly from 300 HV to 550-680 HV after the surface treatment was carried out.

1. INTRODUCTION

Martensitic stainless steels are widely used in applications for which a combination of moderate corrosion resistance and high strength is needed, for example, in components such as propellers, pump impellers, valves and turbines. Owing to the high content of alloying elements, the mechanical strength and corrosion resistance of martensitic stainless steels are very sensitive to heat treatment. Failure of martensitic stainless steels during engineering application due to corrosion, oxidation, friction, fatigue and wear/abrasion is most likely to initiate from the surface because: (i) free surface is more prone to environmental degradation, and (ii) intensity of externally applied load is often highest at the surface[1]. The engineering solution to minimize or eliminate such surface initiated failure lies in tailoring the surface composition and/or microstructure of the near surface region of a component without affecting the bulk[2-4].

Martensitic stainless steels are usually received in the annealed state and then hardened by surface modification via phase transformation[5]. In this regard, the more commonly practiced conventional surface engineering techniques like galvanizing, diffusion coating, carburizing, nitriding and flame/induction hardening possess several limitations like high time/energy/material consumption, poor precision and flexibility, lack in scope of automation/improvisation and requirement of complex heat treatment schedule. Furthermore, the respective thermodynamic and kinetic constraints of restricted solid solubility limit and slow solid state diffusivity impose additional limitations of these conventional or near-equilibrium processes[1,3]. In contrast, the surface engineering methods based on application of electron, ion and laser beams are free from many of the limitations of equilibrium surface engineering methods.

Among the notable advantages, laser surface engineering (LSE) enables delivery of a controlled quantum of energy (1–30 J/cm2) or power (10^4–10^7 W/cm2) with precise temporal and spatial distribution either in short pulses (10^{-3} to 10^{-12} s) or as a continuous wave (CW). The process is characterized by an extremely fast heating/cooling rate (10^4–10^{11} K/s), very high thermal gradient (10^6–10^8 K/m) and ultra-rapid re-solidification velocity (1–30 m/s)[1,3,6-8]. These extreme processing conditions very often develop an exotic microstructure and composition in the near surface region with large extension of solid solubility and formation of metastable/amorphous phases.

1.1. Laser Surface Engineering

Figure 1 presents a brief classification of different LSE methods that involve mainly two types of processes. The first type is meant for only microstructural modification of the surface without any change in composition (hardening, melting, remelting, shocking, texturing and annealing), while the other requires both microstructural as well as compositional modification of the near-surface region (alloying, cladding etc.)[1, 6-8].

The results of the laser hardening process depend primarily on the beam irradiance on the surface of the workpiece, the processing rate and the thermo physical properties of the material. The processing rate in laser hardening can be more usefully expressed as the interaction time, defined for a continuous process as the length of time taken for the laser spot to travel one diameter relative to the work piece[2]. A low interaction time and a high power results in a shallow hardening depth whereas the converse results in a deeper hardening depth. However, the higher peak temperatures and cooling rates required for short processing times may result in the formation of unacceptable quantities of retained austenite[7,8] in steels.

The domain for different laser material processing techniques as a function of laser power and interaction time is illustrated in Figure 2[7,8-10]. The processes are divided into three major classes, namely involving only heating (without melting/vapourizing), melting (no vapourizing) and vapourizing.

1.2. Mechanism of Laser Surface Engineering

The principle mechanism of LSE is the structural phase transformation (i.e. either microstructure & composition together or anyone of them) resulting in the formation of constituents of high hardness. For LSE, characteristic rate to supply and remove heat is 10^6-10^{10} K/s. When the energy, beam diameter, and the scan rate are adjusted to surface modification (i.e. involve change of Phase or state), on self quenching by conduction into the cold material beneath the surface transforms to martensite. This technique gives a hard, wear resistant surface with less distortion than that caused by flame or induction hardening[9,11-12]. The laser surface melting (LSM) is based on rapid scanning of the surface with a beam focused to a power density scale of 10^4 W/cm^2 to 10^7 W/cm^2. Quench rates up to 10^8-10^{10} K/sec provide the formation of fine structures, the homogenization of microstructures, the extension of solid solubility limits, formation of non equilibrium phase and amorphous phases or metallic glasses, with corrosion resistance 10-100 time higher compared to crystalline[12-13]. Schematic mechanism of Laser Surface Melting (LSM) is shown in Figure 3.

Among the different types of laser surface treatment processes, LSM and LTH are the simplest as no additional materials are introduced, and they are especially effective for processing ferrous alloys with grain refinement and increase of the Cr content in solid solution. In fact these processes have been employed for improving the cavitation erosion and/or corrosion resistance of a number of ferrous alloys[7, 14-15]. The degree of enhancement depends on the final

microstructure formed, which in turn depends on the material under treatment and on the laser processing parameters.

The important processing parameters for laser surface heat treatment include the laser beam power, focused laser beam diameter, distribution of power (or heat intensity distribution) across the beam, absorptivity of the beam energy by the work surface, scanning velocity (or longitudinal) of the laser beam and traverse or cross) feed of the laser beam across the substrate surface, and the thermal properties of the work material. The dependent variables are the depth of hardening, geometry of the heat affected zone (HAZ) and its microstructure, and the properties and performance of the resulting heat treated material in service. For a better appreciation of the laser heat treatment process and a wider application of it in industry, it is necessary to establish appropriate relationships between the output variables and the input parameters. It is also necessary to know the operating range of these parameters for laser surface hardening of steels for proper application in industry[16-17].

For surface treatment of metals, CO_2 lasers are most often used since they can provide high powers of the laser beam. CO_2 laser-beam light, however, is characterised by a comparatively long wavelength, 10.6 μm, which in the interaction with the metal surface at the ambient temperature can ensure only up to 5% of energy absorbed. A higher efficiency of laser treatment, however, can be achieved by increasing the laser-beam absorption; therefore, absorbing coatings are frequently used in practical applications[18].

A drawback of laser hardening is that it may be necessary to make multiple passes with the laser over the surface of the workpiece if the beam spot size is not large enough to cover the entire area. Lateral heat flow into the previously hardened track may cause 'back tempering' which can reduce the hardness in the affected area considerably[19].

X20Cr13 German graded martensitic stainless steel (UNS S42000) has chromium content (13%) and low carbon content (0.2%), and it possesses the best mechanical strength among the martensitic grades, which is extensively used as turbine blade material for hydro power plants with BHEL, India. It can be heat treated to achieve a high hardness, which is well known as an important factor in determining the cavitation erosion resistance of a material[5, 19-23].

The aim of the present study was to employ laser surface melting to improve the hardness of X20Cr13. The effect of the laser power, laser scanning speed and pre-hardening surface condition on the hardness, microstructure and geometry was investigated.

2. EXPERIMENTAL DETAILS

2.1. Materials and Sample Preparation

As-received X20Cr13 martensitic stainless steel with nominal composition in wt.%: 13 Cr, 0.5 Ni, 0.5 Mn, 0.2 C,0.3 Si, balance Fe, was prepared as samples for laser surface treatment. To study the effect of surface condition on the hardening characteristics, the samples were subjected to sandblast to improve the roughness and few more samples are coated with Japan black paint to minimize reflection of radiation during laser processing. Laser surface modification was performed using a high-power CW CO_2 laser, with argon flowing at 20 l/min as shielding gas, to minimize oxidation. Preliminary trials with different values of laser power P, and scanning speed v with constant laser spot diameter d at 11.6mm were carried out to determine the processing conditions suitable for surface modification. The criteria used were (i) the laser power density equivalent to melting with interaction time equivalent to transformation hardening as shown in the figure 4 and (ii) the surface hardness of the hardened layer should exceed 600 HV. While preparing the experimental plan, the results stated by A. Camoletto *et*

al.[22] and N.D. Pandey *et al.*[23] were considered. The set of 12 experiments were planned at various combinations of laser processing parameters (as shown in Table 1) were chosen for further investigation of the surface modification of X20Cr13 martensitic stainless steel.

2.2. Macroscopic analysis

To study the macroscopic features of the laser treated zones, the surface topology of treated specimens were observed using stereo microscope at 12X magnification. The cross sectional view of laser treated samples also observed at 12X, 25X, and 40X. The roughness measurement carried out using the "SURF TEST 211 series 178" model machine in both (i.e., longitudinal and transverse) directions of laser treated track. The hardness measurements were carried out using Vickers hardness testing machine.

2.3. Metallographic and Microscopic analysis

After laser treatment the samples were polished and etched with villela's reagent (1 g of Picric acid, 5 ml of HCl and 100 ml of Methanol). The average thickness of the laser transformation-hardened layer was determined by optical microscope at 100X magnification. The microstructure of the hardened layer was analyzed by SEM and optical microscopy. The phases present in the surface layer were determined by XRD using CuK_{α} radiation. A Vickers microhardness was measured under a load of 100 g.

3. RESULTS AND DISCUSSIONS

3.1. Macroscopic analysis

The top surface of the each laser treated track of specimen was observed on a stereomicroscope at 12X magnification. The topology of the samples is shown in Figure 5 and the Stereo microscopic observation of mounted specimens at 25X is shown in Figure 6. It has been found that smoothness (uniformity) of top surface of laser treated specimen increases with increase of hardening (scanning) speed and decreases with the increase in laser powers. Visual examinations revealed that the sand blasted specimens resulted in better surface compared to painted surfaces at all the hardening (scanning) speeds.

The surface roughness are measured in two directions (i.e. longitudinal and traverse) on the top surface of laser treated area are given in Table 4.1 and graphically can be shown in Figure 7. That, a decrement in roughness values has been observed with the increase in hardening (scanning) speed and increases with the increase in power during the range of processing parameters. If the surface conditions can be noticed that, the paint coating is more preferable at high hardening (scanning) speeds, because it results in smaller roughness values in both directions.

3.2. Microstructural Characterization

Microstructure as observed under optical microscope of various hardened zones and the base metal are shown in Figure 8. The Figure 8(a) depicts base metal in as received condition. It contained martensite in tempered condition. The various zones in the laser treated area are schematically shown in Figure 8(b). The melt zones have cast structure consists the dendrites and chilled grains. The fine chilled grains are concentrated near to surface, and going far from melt surface the specimen have dendritic structure as show in Figure 8(c). The interface of the two zones was observed as shown in Figure 8(d & e) giving the schematic difference between the melt zone and HAZ. The HAZ has relatively fine structure in comparison of Base Metal and Melt zone.

Figure 9 shows SEM micrographs of the microstructures of as-received, meltzone and HAZ of laser treated X20Cr13 samples. The phases present in the surface layers of these samples, as identified using the XRD spectra shown in Fig. 10-12. It should be noted that for the CuK_{α} wavelength (0.15406 nm), only a thin layer of approximately 10 μm thick contributes to diffraction. Thus, the phases detected were those present in the treated area.

The SEM micrograph in Fig. 9(a) shows that the sample in the as-received condition (X20Cr13) contained a high density of coarse carbides in a matrix, the matrix being identified as ferrite (α) by XRD. When the temperature was raised by laser, the surface got melted.

When the samples cooled down, martensite (α'), retained austenite (γ_R) and finer carbides were formed. The presence of retained austenite in martensitic stainless steels is common in conventionally heat-treated samples[24] and in laser-treated samples[25] . The amount of retained austenite depends on the alloy composition, especially the carbon content, and the thermal history[26]. An approximate estimation from the peaks in the XRD spectra shown in Figure 10 (b) and (c), the laser treated samples contain retained austenite content[5]. The authors[5, 15, 27-28] are calculated the amounts of retained austenite with respect to laser scanning speed.

The hardness values were measured at the surface of laser treated specimens using the Vickers hardness tester. The variation in hardness as a function of hardening (scanning) speed is shown in Figure 11.

For black Japan paint coated specimens, hardness on the top surface of laser treated slightly dropped with increase in hardening (scanning) speed. However, for sand blasted specimens there was minimal change in hardness with the change in hardening speed in the present work regime, when compare with paint coated samples.

The Microhardness profile along the depth of the laser treated samples is shown in Figure 12. The depth and width of the melt zone and HAZ in the laser treated specimen using optical microscope at 100X magnification. All measurements showing the decrement in depth and width with increase in laser hardening (scanning) speed, increment with increment in laser power.

4. CONCLUSIONS

From the present study on Laser Surface Modification (Melting) of X20Cr13 steel and role of various laser processing parameters namely Laser Power (P), Hardening (scanning) speed, pre-hardening surface condition on hardening characteristics following conclusions can be drawn.

I. Laser Surface Modification results in Microhardness in the range of 550 to 680 VHN, upto the depth of 0.6 mm. After this depth, in HAZ the hardness drops to 480-520 VHN level upto 1.75mm.

II. The pre-hardening surface condition of specimens has influence on the final hardness of the laser treated specimens. Sand blasted specimens have shown moderate values in hardness whereas Japan Black Painted have results in higher values. There is a gradual drop in hardness with increase in hardening speed for painted samples.

III. XRD examination revealed that, the laser treated zones at both conditions of pre hardening surface modification (sand blasted and black Japan paint coated), has the peaks for Martensite and retained austenite. The base metal (X20Cr13 H&T) in as received condition has tempered Martensite, which corresponds to Body Centered Tetragonal peaks in the XRD pattern.

IV. The sample (2.5kW, 10 $mm.s^{-1}$ and Painted)) could be shown higher hardness values with a matrix having a microstructure composed of martensite and retained austenite, and finer carbides. Such a microstructure will be suitable for resistance against erosion with favorable combination of strength and toughness[5].

REFERENCES

1. Molian P A 1989 *Surface modification technologies-An engineers guide* (ed.) T S Sudarshan (NewYork: Marcel Dekker) p. 421
2. Mordike B L 1993 *Materials science and technology* (eds) RW Cahn, P Haasen, E J Kramer (Weinheim: VCH) 15: 111
3. Draper CW, Poate J M 1985 *Int. Met. Rev.* 30: 85–108
4. Draper CW, Ewing C A 1984 *J. Mater. Sci.* 19: 3815
5. K.H. Lo, F.T. Cheng, H.C. Man, *Surf and Coatings Tech* 173 (2003) 96–104
6. J Dutta Majumdar and I Manna *S¯adhan¯a* Vol. 28, Parts 3 & 4, June/August 2003, pp. 495–562.
7. J.F. Ready, *LIA Hand book of Laser Material Processing*, Laser Institute of America, 2001.
8. SteenW M *Laser material processing* Springer Verlag, NewYork 1991
9. E.M.Brenian and B.H. Kear; in M. Bass, ed., *Laser material processing* 1983
10. W. Amende; Barry L. Mordike (ed.) *Laser Treatment of Metals*, DGM Informatics 1987
11. M.F.Ashby and K.E. Easterling, *Acta Metallurgica.,* 32 (1984), p.1935
12. S.T. Picraux, *Phys. Today,* Nov. 1984, p.38
13. Stjepan Lugomer *Laser technology: Laser Driven Processes*, Prentice-Hall Inc., New Jersey 1990.
14. K.H. Lo, F.T. Cheng, C.T. Kwok, H.C. Man, *Materials Letters* 58 (2003) 88– 93.
15. C.T. Kwok, H.C. Man, F.T. Cheng, *Surf. Coat. Technol.* 126 (2000) 238–255.
16. R. Komanduri, Z.B. Hou, *International Journal of Machine Tools & Manufacture* 44 (2004) 991–1008.
17. J. Mazumber, *Journal of Metals*, Vol.35 (5) May 1983 pp. 18-26.
18. J. Grum, T. Kek, *Thin Solid Films* 453 –454 (2004) 94–99.
19. E. Kennedy, G. Byrne, D.N. Collins, *Journal of Materials Processing Technology* (2004) article in press.
20. S. Vaidya, C.M. Preece, *Metall. Trans. A* 9 (1978) 299–307.
21. K.F. Tam, F.T. Cheng, H.C. Man, *Surf. Coat. Technol.* 149 (2002) 36–44.
22. A. Camoletto, G. Malino and S. Talentino *Materials and Manufacturing processes*, 6(1), 1991, pp.53-65.
23. N.D. Pandey, K.Venugopal and A. Bharti, "Laser Hardening of Steam Turbine Blades", unpublished *DMRL Technical Report* (2003)
24. G.F.V. Voort, H.M. James, *Wrought stainless steels, Metallography and Microstructures, Metals Handbook, vol. 9,* ASM, Metals Park, OH, USA, 1985, pp. 279–296.
25. R. Colaco, R. Vilar, *Scr. Mater.* 36 (1997) 199–205.
26. R. Colaco, R. Vilar, *Scr. Mater.* 41 (1999) 715–721.
27. R. Colaco, R. Vilar, J. *Mater. Sci. Lett.* 17 (1998) 563–567.
28. K. Obergfell, V. Schulze, O. Vo¨hringer, *Materials Science and Engineering A*355 (2003) 348 – 356

TABLES

Table 1. Laser process parameter combination for experimental studies

Run	Power (kW)	Speed ($mm.s^{-1}$)	Surface condition
1	2.5	10	Sand
2	3.5	10	Sand
3	2.5	20	Sand
4	3.5	20	Sand
5	2.5	40	Sand
6	3.5	40	Sand
7	2.5	10	Paint
8	3.5	10	Paint
9	2.5	20	Paint
10	3.5	20	Paint
11	2.5	40	Paint
12	3.5	40	Paint

FIGURES

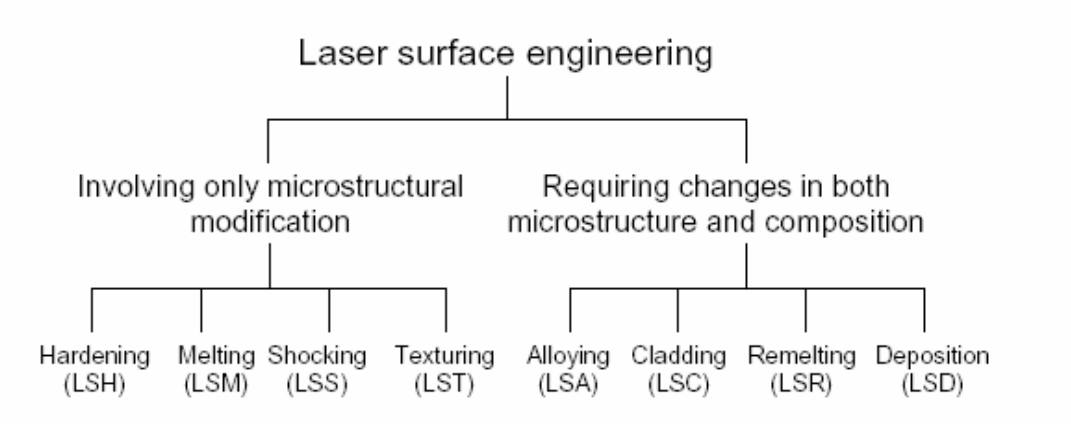

Figure 1. General classification of Laser Surface Engineering (LSE)

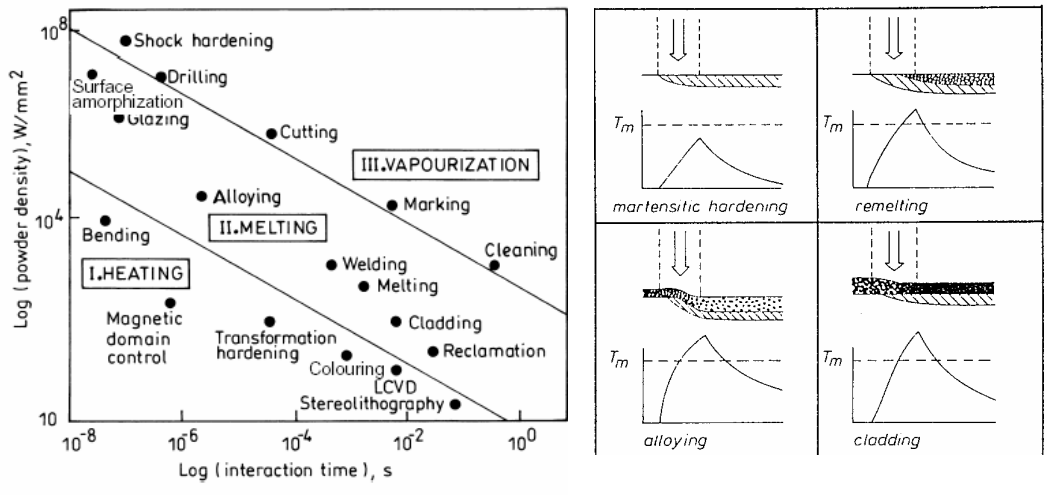

Figure 2. Process map (schematic) in terms of laser power density as a function of interaction time for different examples of Laser Material Processing [1 from 9]

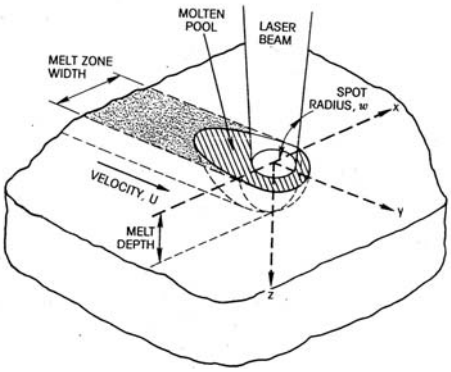

Figure 3. Schematic of a laser beam – substrate geometry during rapid surface melting and solidification

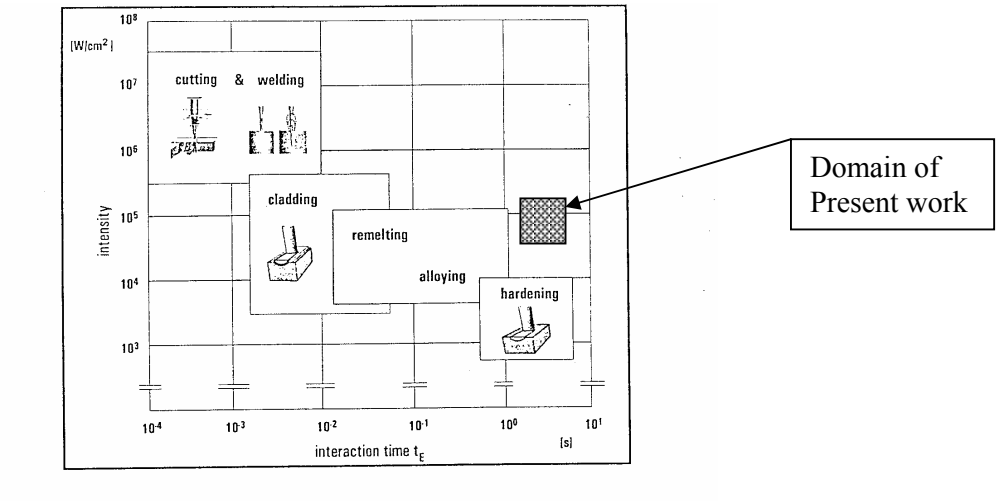

Figure 4. Schematic representation of present work process regime

Stereo Microscopic observation of Laser Surface Treated Specimen Topology at 12 X					
2.5kW Sand blasted surface condition			2.5kW Japan Black Painted surface condition		
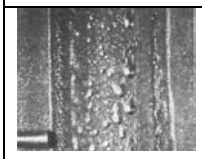	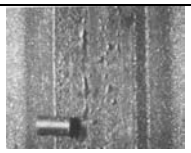	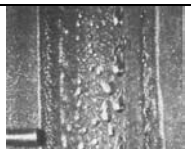			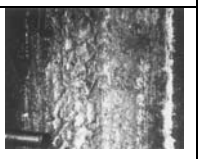
$10mm.s^{-1}$	$20mm.s^{-1}$	$40mm.s^{-1}$	$10mm.s^{-1}$	$20mm.s^{-1}$	$40mm.s^{-1}$
3.5kW Sand blasted surface condition			3.5kW Japan Black Painted surface condition		
	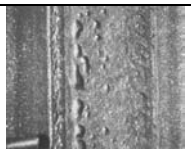	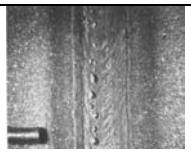	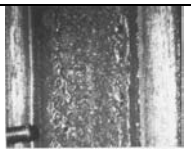		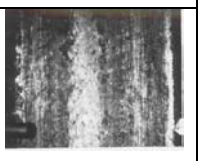
$10mm.s^{-1}$	$20mm.s^{-1}$	$40mm.s^{-1}$	$10mm.s^{-1}$	$20mm.s^{-1}$	$40mm.s^{-1}$

Figure 5. Stereo microscopic observation of top surface of laser treated specimen Surface, 12X magnification

Stereo microscopic observation of mounted specimens				
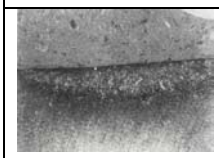	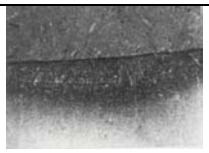	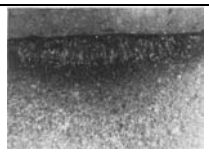	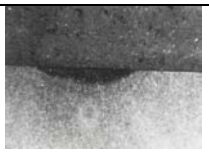	
$10mm.s^{-1}$, Paint 2.5kW, 25X	$10mm.s^{-1}$, Sand 3.5kW, 25X	$10mm.s^{-1}$, Paint 3.5kW, 25X	$40mm.s^{-1}$, Sand 2.5kW, 25X	$40mm.s^{-1}$, Paint 3.5kW, 25X

Figure 6. Stereo microscopic observations of mounted specimens at 25X

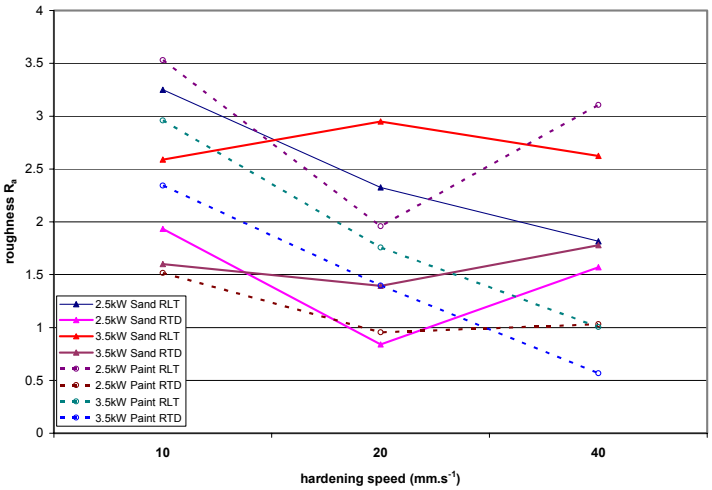

Figure 7. The plot for roughness values (R_{LT} and R_{TD}) in against of hardening speed

Optical microscopic observation				
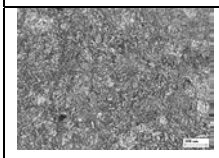	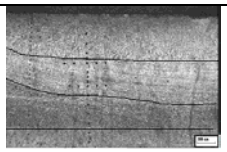		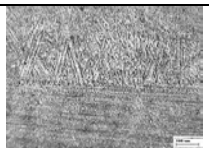	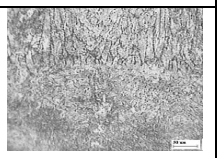
(a) Base metal as in received state 100X	(b) Various zones in laser treated area 50X	(c) Various zones in laser treated area 100X	(d) interface of melt zone and HAZ at 100X	(e) interface of melt zone and HAZ at 200X

Figure 8. Microstructural observation using Optical Microscope

Scanning Electron microscopic (SEM) observation		
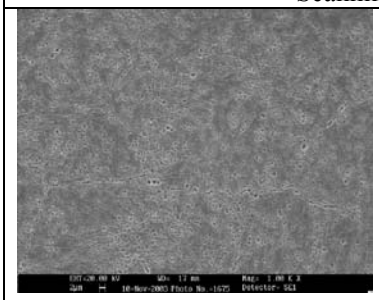	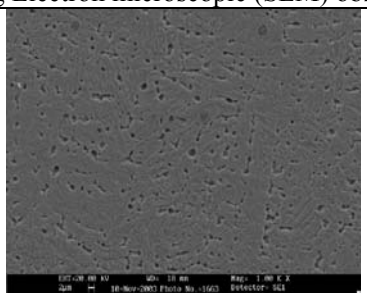	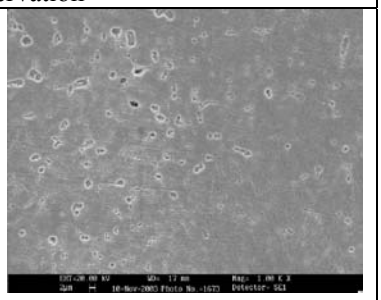
(a) Base metal as in received state 1000X	(b) melt zone at 1000X magnification	(c) Heat Affected zone at 1000X magnification

Figure 9. Scanning Electron microscopic (SEM) observation

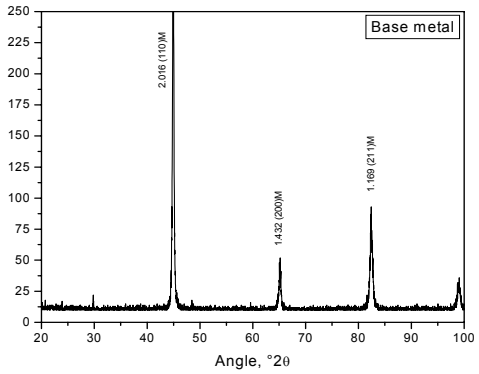

Figure 10(a) Base metal as in received state

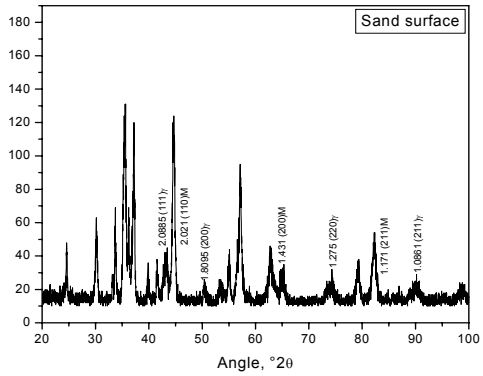

(b) Laser treated with Sand blasted surface

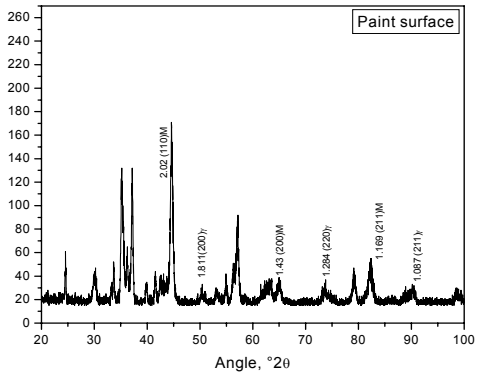

10 (c) Laser treated with painted surface

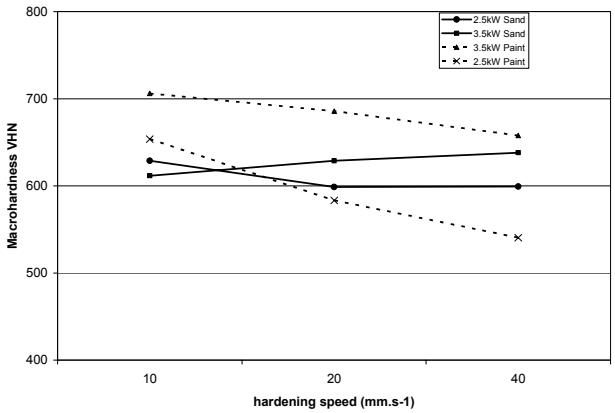

Figure 11. The plot of Macrohardness values against laser hardening speed

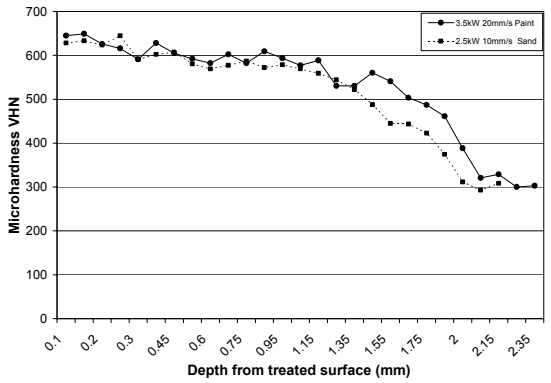

Figure 12. The plot of Microhardness profile against depth of laser treated layer